JOURNAL OF SOLID STATE CHEMISTRY **140,** 278–284 (1998)
ARTICLE NO. SC987887

Nickel Oxidation State and Magnetic Properties of Hole-Doped and Reduced $Nd_{2-x}Sr_xNiO_y$ Compounds

M. Jiménez-Ruiz, C. Prieto,[1] J. L. Martínez, and J. M. Alonso

Instituto de Ciencia de Materiales de Madrid, Consejo Superior de Investigaciones Científicas, Cantoblanco, E-28049 Madrid, Spain
E-mail: cprieto@icmm.csic.es

Received November 7, 1997; in revised form May 11, 1998; accepted May 12, 1998

The Ni *K*-edge XANES of reduced $Nd_{2-x}Sr_xNiO_4$ samples shows an increase of Ni^{3+} content with Sr^{3+} concentration. The appearance of mixed valence Ni^{2+}/Ni^{3+} produces a change in the magnetic properties of the system. The Nd^{3+} sublattice orders antiferromagnetically at $T_N \sim 13$–20 K for $x = 0.4$, 0.5, and 0.6, due to the interactions of Ni–Nd sublattices. For $x = 0.8$ this order begins to disappear because of the effect of the low spin state Ni^{3+} created at the NiO_4 planes. Additionally, the reduced family $Nd_{2-x}Sr_xNiO_y$ ($y < 4$) shows the disappearance of Ni^{3+}, the decrease of Ni^{2+} with respect to the nonreduced form, and the appearance of Ni^{+}. All the compounds of the reduced family show AF order at low temperature.

1. INTRODUCTION

Due to the similarity between Ln_2NiO_4 and La_2CuO_4, the study of hole-doped $Nd_{2-x}Sr_xNiO_4$ may help to understand the superconductivity mechanism. The electronic and structural properties of $Ln_2NiO_{4+\delta}$-type compounds have been reported to be very sensitive to oxygen stoichiometry (1–3). Neutron diffraction measurements on $Nd_2NiO_{4+\delta}$ (2) showed that the oxygen stoichiometry is critical for three-dimensional magnetic order because an oxygen excess creates structural defects, which prevent the magnetic order. For this reason it is interesting to study electron-doped $Nd_{2-x}Sr_xNiO_y$ compounds. All these samples crystallize with K_2NiF_4-type structure, whose structural characteristic is that the NiO_6 octahedral units share corners in the *ab* plane.

In particular, in this paper, we study the hole- and electron-doped Nd_2NiO_4 family, in which holes are introduced by an oxygen excess and by substitution for the trivalent rare earth by a divalent cation (Sr^{2+}), and electron doping is introduced by a reduction process of the previous compounds. The aim of our work is to relate the Ni valence state to the macroscopic magnetic properties. In the following, we will present separately the hole-doped $Nd_{2-x}Sr_xNiO_4$ samples and the electron-doped $Nd_{2-x}Sr_xNiO_y$ (with $y < 4 - x/2$) samples.

(i) The structural changes produced in the $Nd_{2-x}Sr_xNiO_4$ system have been studied by X-ray and electron diffraction (4), which indicate that for $x = 0.2$ the system undergoes to a structural transition from *Fmmm* (orthorhombic) to *I*4/*mmm* (tetragonal). In both structures, Ni atoms remain octahedrally coordinated (NiO_6).

From X-ray absorption near-edge structure (XANES) spectroscopy, information can be obtained regarding the electronic ground state. On the other hand, changes of the threshold energy can also give information about the differences in the electronic configurations of the ground state and about the formal valence of the absorber atom. Kuiper *et al*., based on O *K*-edge XANES in the $La_{2-x}Sr_xNiO_4$ family (5), showed that doping holes have O2*p* character, while the Ni *K*-edge XANES analysis of the same family indicates that these holes have a mixed O2*p* and Ni3*d* character (6). On the other hand, a comparison between Ni *K*-edges of NiO and $NdSrNiO_4$ compounds has been carried out by Tan *et al*. (6). This result demonstrates that the doped holes have a substantial amount of Ni3*d* character (30–40%).

These holes introduced in the Ni bands produce changes in the electrical and magnetic properties. The magnetic properties of some $Nd_{2-x}Sr_xNiO_{4+\delta}$ compounds have been studied by magnetic susceptibility measurements (7, 8) and by a.c. susceptibility and resistance measurements (9). These studies show that at high temperatures all the compounds of this family have Curie–Weiss behavior and, at low temperatures, some members of the family have an antiferromagnetic (AF) long range magnetic order (LRMO) of the Nd sublattice (the x range found by several authors varies: $0.3 \leq x \leq 0.8$ in Refs. (7, 8) and $0.3 \leq x \leq 0.9$ in Ref. (9)). Additionally, the $Nd_{1.5}Sr_{0.5}NiO_4$ compound has been studied in detail by magnetic susceptibility and neutron diffraction measurements (10). The combination of both techniques indicates that, at 45 K, the Ni sublattice has AF

[1]Author to whom correspondence should be addressed.

0022-4596/98 $25.00

short range magnetic order (SRMO) and, at 11 K, the SRMO of the Ni sublattice coexists with the LRMO of the Nd sublattice, in such a way that the magnetic order is due to the coupling between both sublattices.

(ii) The structural changes in the $La_{2-x}Sr_xNiO_y$ ($0 \leq x \leq 0.8$, $3.38 \leq y \leq 4$) reduced family have also been studied by X-ray and electron diffraction (4). All members of this family present monoclinic symmetry with $B112/n$ spatial group (*Cmca* and $C2/c$ in the standard setting) for $3.8 \leq y \leq 4$ and orthorhombic symmetry with *Immm* spatial group for $3.45 \leq y \leq 3.75$ (11). The existence of twin domains due to different rotation axes of the octahedra has been observed. Neutron diffraction data (12) show that anionic vacancies are mainly concentrated at the twin boundaries, so the Ni atoms are in a square planar environment (NiO_4) and the oxidation state should be lower than $+2$, therefore changing the magnetic properties.

The magnetic properties of this system have been also studied by susceptibility measurements (8) and a detailed study of the $Nd_{1.8}Sr_{0.2}NiO_{3.72}$ sample has been carried out by Medarde *et al.* (13), who show by neutron diffraction experiments that the Nd^{3+} sublattice orders antiferromagnetically at 13.5 K. The Ni^{2+} sublattice has an AF order at 320 K and two spin reorientations of the Ni^{2+} sublattice have been observed at 130 and 13.5 K. On the other hand, the susceptibility data (12) indicate the presence of a ferromagnetic component below 70 K. The study of all the samples belonging to the reduced family (8) shows an AF order of the Ni sublattice at 330 K and of the Nd sublattice at a temperature between 5 and 17 K, depending on the compound.

In order to study the variation of the Ni valence in both systems we have performed X-ray absorption experiments at the Ni *K*-edge, where, by tuning the X-ray energy, it is possible to obtain the fine structure at and above the absorption edge of the selected atom. From XANES spectroscopy, which includes the pre-edge structure and the multiple scattering processes, it is possible to obtain information about the oxidation state of the absorber atom and its stereochemical environment. After that, we will correlate the Ni valence information obtained from the XANES experiments with the macroscopic magnetic properties of the systems.

2. EXPERIMENTAL

$Nd_{2-x}Sr_xNiO_{4+\delta}$ samples were synthesized by the ceramic method from stoichiometric amounts of Nd_2O_3, $SrCO_3$, and NiO heated at 1250°C for 100 h. After being ground, the samples were fired in air at 1400°C for 200 h. The reduced samples were obtained by heating the oxidized precursor at moderate temperatures (380°C) in a controlled dry H_2 atmosphere for 15–24 hours and cooled to room temperature inside the furnace while the H_2 flow was maintained. The cationic composition of all the samples was determined by inductive coupling plasma spectrometry (ICP) and the Ni concentration by iodometric titration. Oxygen content determination was performed by means of a thermogravimetric analysis system (TGA) developed on the basis of a Cahn D-200 electrobalance.

X-ray absorption experiments were carried out at the XAS-3 beamline at the DCI storage ring (LURE) with an electron beam energy of 1.85 GeV and an average current of 250 mA. Data were collected using a fixed exit monochromator with two flat Si (311) crystals, and detection was made using two gas filled ion chambers. Energy resolution was estimated by the Cu foil 3*d* near-edge feature to be about 2 eV. The energy calibration was monitored using the Cu foil sample; it was taken as 8993.9 eV at the first maximum above the edge. Magnetic susceptibility was measured in a SQUID magnetometer (MPMS-5S from Quantum Design) in a temperature range from 1.7 to 400 K and an applied magnetic field up to 50 kOe.

3. RESULTS AND DISCUSSION

3.1. $Nd_{2-x}Sr_xNiO_4$ ($0.2 \leq x \leq 0.8$) Hole Doped Samples

Figure 1 shows the Ni *K*-edge XANES spectra of the samples with nominal extreme values in hole concentration. These samples could be considered representative of the nonreduced system $Nd_{1.7}Sr_{0.3}NiO_4$ and $Nd_{1.2}Sr_{0.8}NiO_4$, where the expected concentrations of Ni^{3+} could be 33% and 80%, respectively, calculated on the basis of charge compensation, and only divalent and trivalent Ni ions are allowed. The evolution of the normalized XANES spectra at the Ni *K*-edge for increasing Sr content has been

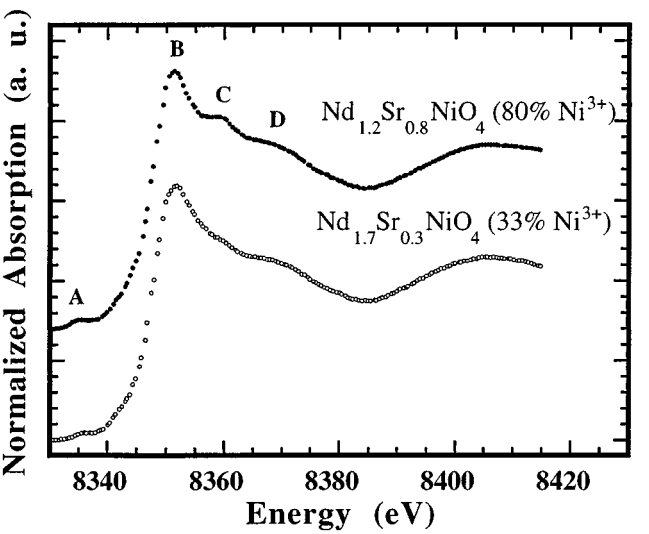

FIG. 1. Normalized XANES spectra at Ni *K*-edge of $Nd_{1.7}Sr_{0.3}NiO_4$ and $Nd_{1.2}Sr_{0.8}NiO_4$ samples.

reported in Ref. (14). The evolution, when x increases, can be summarized as follows:

(a) An increase of the prepeak (A feature) corresponding to the $1s \rightarrow 3d$ transition. This is a forbidden dipolar transition for an absorber with inversion symmetry; however, the quadrupolar one is permitted. In these compounds, the octahedra distortion is very small, so on average the local inversion symmetry is preserved (15). For this reason the increase of this prepeak has an electronic origin rather than a structural one, since the empty $3d$ density of states increases. The increase of the A feature as the Ni oxidation state increases is in agreement with the theoretical calculations for the XANES spectra for other similar compounds. For example, it has been reported for $LaNiO_3$ and $NdNiO_3$ (16), where, based on multiple scattering theory and using a self-consistent field for the final state potential and charge density, it can be concluded that this prepeak represents the transition between the $1s$ shell and the hole in the oxygen p band. Thus, it is directly related to the presence of the $3d^8L$ electronic configuration in the ground state.

(b) The B and D features are present in every compound. They are characteristic of the Ni^{2+} and they are associated with $|3d^9L\rangle \rightarrow |c3d^9L4p^1\rangle$ and $|3d^8\rangle \rightarrow |c3d^84p^1\rangle$ transitions, respectively.

(c) The fundamental state of Ni^{3+} can be described as a mixed configuration of $|3d^7\rangle$ and $|3d^8L\rangle$ states. The C-feature corresponds to the $|3d^8L\rangle \rightarrow |c3d^8L4p^1\rangle$ transition, and it has been observed in $LnNiO_3$ ($Ln =$ rare earths) compounds (where the Ni valence is $3+$ by Medarde *et al.* (17); therefore we can conclude that in our samples some Ni^{3+} amount appears to compensate the charge, because this feature is absent in compounds with only divalent Ni. Moreover, reinforcing this conclusion, the self-consistent calculations reported by García *et al.* (16) show that the C-feature is only present in the calculated spectrum of these compounds when it is considered the second shell which is formed by eight lanthanum atoms around the Ni^{3+} (NiO_6La_8). The theoretical Ni K-edge XANES spectra of $LaNiO_3$ and $NdNiO_3$ were calculated by using the $Z+1$ approximation for the final state potential and increasing the numbers of shells around the photoabsorber.

Due to the fact that Sr^{2+} and O^{2-} are diamagnetic ions, the contribution to the magnetic susceptibility in the $Nd_{2-x}Sr_xNiO_4$ samples will come from the Ni and Nd ions, so the appearance of mixed valence Ni^{2+}/Ni^{3+}, observed at the Ni K-edge XANES spectra, will have some influence on the macroscopic magnetic properties. Figure 2a shows the magnetic susceptibility of the $Nd_{2-x}Sr_xNiO_4$ ($0.2 \leq x \leq 0.8$) samples under an applied magnetic field of 500 Oe. It is important to note that there are also two samples with oxygen excess δ ($Nd_{1.8}Sr_{0.2}NiO_{4.14}$ and $Nd_{1.75}Sr_{0.25}NiO_{4.04}$ with $\delta = 0.14$ and 0.04, respectively), that have interstitial oxygens. Similar behavior can be expected in

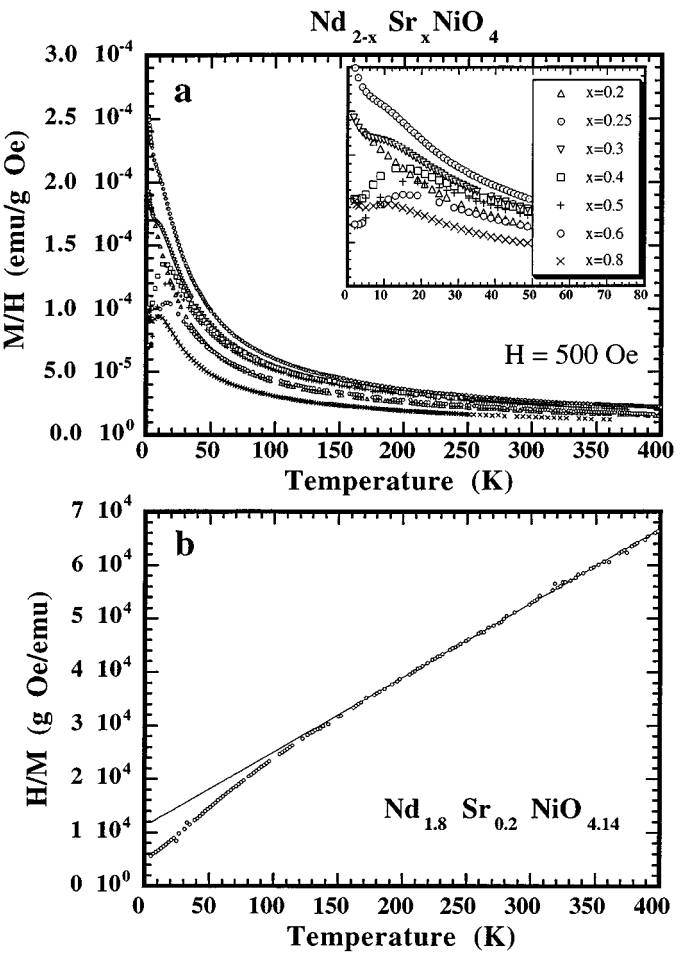

FIG. 2. (a) Magnetic susceptibility under an applied magnetic field of 500 Oe of $Nd_{2-x}Sr_xNiO_{4+\delta}$ family ($\delta = 0.14$ and 0.04 for $x = 0.2$ and 0.25, respectively). (b) Inverse of the magnetic susceptibility of $Nd_{1.8}Sr_{0.2}NiO_{4.14}$ and the corresponding fitting to the Curie-Weiss law. Inset of (a) shows the peak in susceptibility at low temperature.

$Nd_2NiO_{4+\delta}$ samples where the interstitial oxygens create structural defects, which prevent magnetic order at low temperatures (2). For $x = 0.2$ ($\delta = 0.14$) the magnetic susceptibility shows paramagnetic behavior. However, a clear deviation from the linear trend is observed at the inverse of the magnetic susceptibility (Fig. 2b). It can be rationalized as follows: as the Ni sublattice is not ordered, the susceptibility is dominated by the population of the fundamental state of the Nd^{3+} ion, $^4I_{9/2}$. The observed deviation from the linear behavior indicates that there is a depopulation of the crystal field split term $^4I_{9/2}$ when the temperature decreases, as has been reported previously (7).

For $x = 0.25$ and 0.3 samples ($\delta = 0.04$ and 0, respectively) an incipient maximum begins to be observable in the susceptibility, but it does not appear clearly until to a concentration of $x = 0.4$ (40% Ni^{3+}), because for that low a Sr^{2+} concentration, the Ni^{3+} introduced can be

considered an impurity and the J_{Ni-Nd} interaction is not strong enough to antiferromagnetically order the Nd^{3+} sublattice.

Figure 2a shows that a maximum in the susceptibility at a temperature in the 10–20 K range only appears for intermediate Sr^{2+} concentrations ($0.4 \leq x \leq 0.6$). Greedan *et al.* (10) showed that in the $Nd_{1.5}Sr_{0.5}NiO_4$ compound this peak is not related directly to T_N, because at this temperature the SRMO of the Ni sublattice and the LRMO of the Nd sublattice (due to interaction between the Nd and Ni sublattices) are coexisting.

As it can be observed in Fig. 2a, this maximum begins to disappear for $x = 0.8$, probably due to the great amount of Ni^{3+} created in the Ni–O planes: with Ni octahedrally oxygen coordinated, Ni^{3+} is expected to be found in a low spin state ($S = \frac{1}{2}$), so when the Sr^{2+} amount increases in the system, there will be a value of x that creates too many Ni^{3+} in the planes with low magnetic moment ($x = 0.8$ for this system), so the Ni–Nd interactions are weakened and the peak associated with the AF order at low temperature begins to disappear when the quantity of Ni^{3+} is large enough.

In conclusion, the X-ray absorption and magnetic experiments are in agreement: the measured XANES spectra of the $Nd_{1.2}Sr_{0.8}NiO_4$ sample show that Ni^{3+} dominates and the maximum in the susceptibility in the 10–20 K range begins to disappear as a result.

The magnetic susceptibility in the 150–300 K temperature range has been fit to the equation $\chi = C/(T + \theta)$, where C and θ are the Curie and the Weiss constants, respectively. The values obtained are given in Table 1. In this temperature range, the stoichiometric compound (Nd_2NiO_4) shows an AF ordering of the Ni sublattice ($T_N \sim 320$ K) (18). In our samples there is no evidence of such an ordering near 320 K. Thus, the contribution to the susceptibility should be due to the Nd^{3+} sublattice. Figure 3 shows the relevant parameters vs Sr^{2+} concentration: (i) the effective theoretical magnetic moment per atom of Nd, μ_{eff}(theor.); (ii) the experimental one obtained after fitting, μ_{eff}(exp.); and (iii) the difference between them, $\Delta\mu_{eff} = \mu_{eff}(\text{exp.}) - \mu_{eff}(\text{theor.})$.

The theoretical magnetic moment decreases linearly vs Sr^{2+} content, because when x increases, the Nd^{3+} paramagnetic ions are replaced by Sr^{2+} diamagnetic ions. The experimental magnetic moment presents an anomaly for $x = 0.2$ which may be due to the structural transition from the *Fmmm* orthorhombic to the *I*4/*mmm* tetragonal space group. Its dependence on x in the range $0.2 \leq x \leq 0.4$ is similar to the corresponding dependence for the a lattice parameter in this concentration range (4). It can be concluded from this result that the magnetic properties are very sensitive to the Ni–O distances in the basal plane. On the other hand, the experimental magnetic moments are always higher than the theoretical ones, calculated under the assumption that only the Nd^{3+} sublattice contributes,

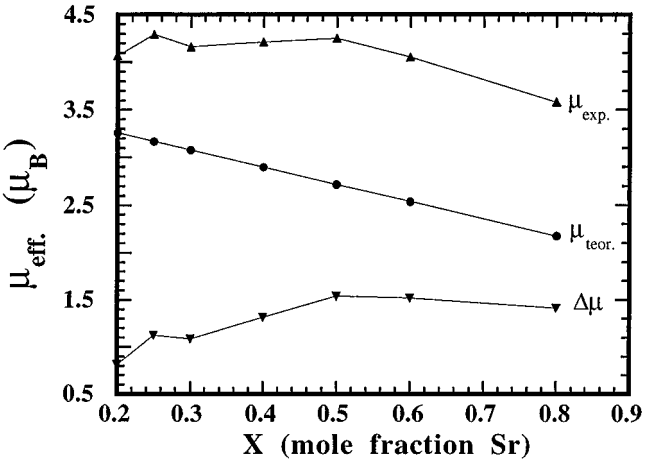

FIG. 3. Variation of the theoretical magnetic moment per atom of Nd μ_{eff} (theor.), the experimental magnetic moment μ_{eff} (exp.), and the difference between them, $\Delta\mu_{eff} = \mu_{eff}(\text{theor.}) - \mu_{eff}(\text{exp.})$, with the percentage of Sr in the $Nd_{2-x}Sr_xNiO_{4+\delta}$ family

because there would be some contribution coming from the Ni sublattice that we did not take into account. The increase of the magnetic moment differences $\Delta\mu_{eff}$ vs x from $x = 0.2$ to $= 0.5$ can be attributed to the presence of Ni^{2+}/Ni^{3+} mixed valence, because the introduction of Ni^{3+} in to the lattice frustrates the AF order of Ni^{2+} sublattice at high temperature.

All the Weiss constants, given in Table 1, remain negative for all these compounds, indicating that the dominant exchange interactions are antiferromagnetic.

3.2. $Nd_{2-x}Sr_xNiO_y$ ($0.2 \leq x \leq 0.5$ and $3.5 \leq y \leq 3.79$) Samples

Ni *K*-edge X-ray absorption studies have been carried out on the reduced family in order to compare their spectra to the nonreduced ones with the same Sr^{2+} content. Figure 4 shows the Ni *K*-edges of two samples, $Nd_{1.6}Sr_{0.4}NiO_y$ with $y = 3.62$ and 4, and their corresponding second derivatives. The same behavior is observed for other samples with different Sr^{2+} content and level of reduction. Several conclusions can be extracted from Fig. 4.

(a) The energy of the B feature for the $y = 3.62$ sample is about 1.5 eV lower than that for $y = 4$. Table 2 gives for each reduction the position of the B feature, the corresponding intensity at this energy, the difference of the B feature energy between the nonreduced and the reduced samples, and the Ni valence. Qualitatively, the edge energy is higher for a more positive absorber (i.e., less well screened), so our results are consistent with a decrease of the Ni oxidation state in the reduced $Nd_{1.6}Sr_{0.4}NiO_{3.62}$ sample in relation to $Nd_{1.6}Sr_{0.4}NiO_4$, in which some Ni^{3+} (40%) appears when the holes are introduced by the Sr^{2+}. The values of the edge

TABLE 1

Theoretical Magnetic Moment per Atom of Nd, μ_{eff}(theor.); Experimental Values Obtained after Fitting the Magnetic Susceptibility to the Curie–Weiss Equation, μ_{eff}(exp.); $\Delta\mu_{eff} = \mu_{eff}$(theor.) $- \mu_{eff}$(exp.); and Weiss Constants Obtained after Fitting, θ(K), for the $Nd_{2-x}Sr_xNiO_4$ Family

Compound	μ_B			
	Nd μ_{eff}(theor.)	μ_{eff}(exp.)	$\Delta\mu_{eff}$(Ni)	θ(K)
$Nd_{1.8}Sr_{0.2}NiO_{4.14}$	3.26	4.07	0.81	−77.0
$Nd_{1.75}Sr_{0.25}NiO_{4.04}$	3.17	4.29	1.12	−77.8
$Nd_{1.7}Sr_{0.3}NiO_4$	3.08	4.16	1.08	−79.6
$Nd_{1.6}Sr_{0.4}NiO_4$	2.90	4.21	1.31	−74.7
$Nd_{1.5}Sr_{0.5}NiO_4$	2.72	4.25	1.54	−77.9
$Nd_{1.4}Sr_{0.6}NiO_4$	2.53	4.05	1.52	−76.0
$Nd_{1.2}Sr_{0.8}NiO_4$	2.17	3.58	1.41	−76.2

TABLE 2

Position of the B Feature of the $Nd_{2-x}Sr_xNiO_4$ and the Corresponding Reduced Sample, E_B (eV); Difference between the Positions for the Same Sr Amount, ΔE_B (eV); Intensity at That Energy, I_B (Arbitrary Units); and Formal Valence of the Ni

Compound	E_B(eV)	ΔE_B(eV)	I_B (arb. units)	Ni valence
$Nd_{1.8}Sr_{0.2}NiO_{4.14}$	8350.5		1.48	2.40
$Nd_{1.8}Sr_{0.2}NiO_{3.79}$	8348.4	2.1	1.40	1.78
$Nd_{1.75}Sr_{0.25}NiO_{4.04}$	8350.4		1.49	2.25
$Nd_{1.75}Sr_{0.25}NiO_{3.76}$	8348.5	1.9	1.38	1.77
$Nd_{1.7}Sr_{0.3}NiO_4$	8349.9		1.49	2.48
$Nd_{1.7}Sr_{0.3}NiO_{3.69}$	8348.4	1.5	1.35	1.68
$Nd_{1.6}Sr_{0.4}NiO_4$	8349.9		1.49	2.40
$Nd_{1.6}Sr_{0.4}NiO_{3.62}$	8348.4	1.5	1.37	1.64
$Nd_{1.5}Sr_{0.5}NiO_4$	8349.5		1.43	2.50
$Nd_{1.5}Sr_{0.5}NiO_{3.52}$	8348.4	1.1	1.33	1.54

energy of the reduced samples (given in Table 2) are always lower than the values corresponding to the nonreduced samples (for the same Sr amount). But comparing the non reduced samples (or the reduced ones), when the Ni valence changes there is not an appreciable variation in the energy threshold, as might be expected. In the nonreduced samples the Ni^{3+} percentage increases with x, while in the reduced samples is the Ni^{+} percentage which increases. The reason could be because the energy shift also depends on the atomic arrangements around the absorber, as has been shown by García *et al.* (19). In our case the small change of the atomic volume of Sr^{2+} with respect to the Nd^{3+} may rearrange the Ni environment.

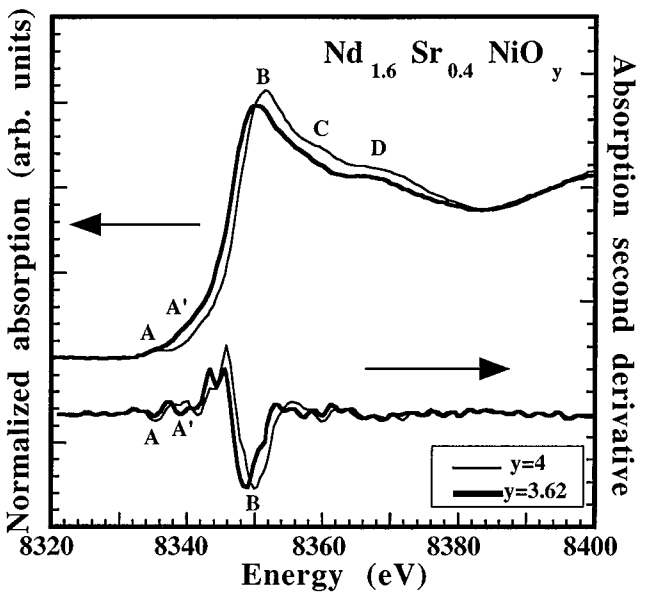

FIG. 4. Normalized XANES spectra at Ni K-edge of $Nd_{1.6}Sr_{0.4}NiO_y$ ($y = 4$ and 3.62) and the absorption second derivative of each spectrum.

(b) The complete disappearance of the C feature, associated with the presence of Ni^{3+}, is observed.

(c) Although the A feature still appears in the reduced one, it has a lower magnitude than that corresponding to the $y = 4$ compound, so there are more Ni3d holes in $Nd_{1.6}Sr_{0.4}NiO_4$ than in $Nd_{1.6}Sr_{0.4}NiO_{3.62}$, which is in agreement with the decrease of the Ni oxidation state for the reduced samples.

(d) The B feature intensity is lower for the $y = 3.62$ than for the $y = 4$ compound. Values given in Table 2 show that this is also the tendency for the samples with the same Sr^{2+} amount. This means that the $|3d^9L\rangle$ configuration (Ni^{2+}) has less weight in the reduced one.

(e) The absorption second derivative of the reduced compound presents an additional minimum at 8339.1 eV (A′ feature) which is not present in the $y = 4$ compound. This feature has been observed at the same energy in plane square coordinated Ni^{+} (20) and corresponds to the $|3d^8 4s^1\rangle \rightarrow |c3d^8 4s^1 4p^1\rangle$ transition. Based upon this, the additional feature could be explained as the presence of Ni^{+} in the reduced compound and additionally a plane square environment can be assumed for these ions. It should be noted that the result of the existence of Ni^{+} in these reduced compounds obtained by XANES spectroscopy is in agreement with those previously obtained in Ref. (4) by iodometric titration analysis.

This change in the Ni state valence of the samples observed by XANES spectroscopy should also be reflected in the magnetic properties. Figure 5 shows the magnetic susceptibility of the reduced system $Nd_{2-x}Sr_xNiO_y$ ($0.2 \leq x \leq 0.6$ and $3.48 \leq y \leq 3.79$) under an applied magnetic field of 500 Oe. A weak maximum corresponding to

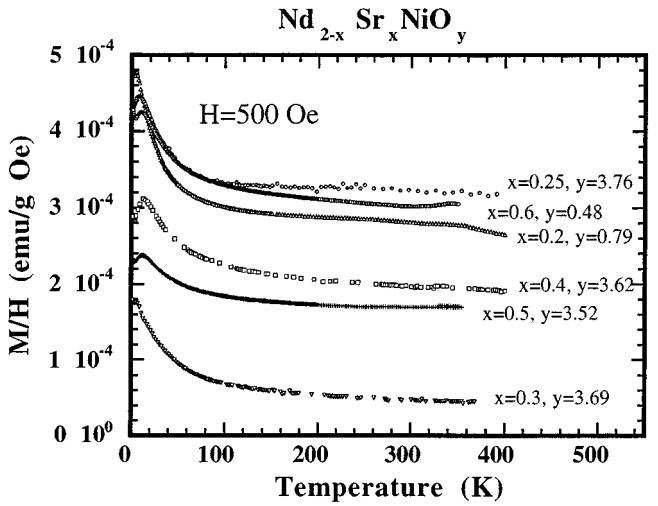

FIG. 5. Magnetic susceptibility under an applied magnetic field of 500 Oe of $Nd_{2-x}Sr_xNiO_y$ family with $0.2 \leq x \leq 0.6$ and $3.48 \leq y \leq 3.79$.

AF order of the Ni^{2+} sublattice appears at $T \sim 330$ K, but in some compounds it is masked by the paramagnetic contribution of the Nd^{3+} sublattice. Another characteristic is the existence of a second maximum at low temperature (5–7 K for $0.2 \leq x \leq 0.3$ and 12–15 K for $0.4 \leq x \leq 0.6$) associated with the 3D AF order of the Nd^{3+} sublattice. A study of $Nd_{1.8}Sr_{0.2}NiO_{3.72}$ showed that this peak also contains the contribution of the Ni^{2+} sublattice spin reorientations as observed by neutron diffraction data (8).

It can be observed in Fig. 5 that the magnetic susceptibility of the samples is above a different background for each sample. This is due to a weak ferromagnetic contribution that arises from some metallic Ni impurity precipitated during the sample reduction process. Metallic Ni orders ferromagnetically at $T_C \sim 630$ K, so in the temperature range of the measurements its contribution can be considered a constant. The percentage of impurity in the samples has been calculated by subtracting the background from the susceptibility data and with the saturation magnetization value of the metallic Ni ($M_s = 0.62\ \mu_B$). The percentage varies from 0.02% to 0.26% of metallic Ni in $Nd_{1.7}Sr_{0.3}NiO_{3.69}$ and $Nd_{1.75}Sr_{0.25}NiO_{3.76}$, respectively.

4. CONCLUSIONS

We have performed Ni *K*-edge XANES and magnetic susceptibility measurements in $Nd_{2-x}Sr_xNiO_4$ ($0.2 \leq x \leq 0.8$) and $Nd_{2-x}Sr_xNiO_y$ ($0.2 \leq x \leq 0.5$ and $3.5 \leq y \leq 3.79$) samples in order to determine the Ni oxidation state and its influence on the magnetic properties of the system. The Ni *K*-edge XANES study of the first system shows qualitatively an increase of the amount of Ni^{3+} as x increases. This change in the Ni oxidation state affects to the magnetic properties in the following way: The $x = 0.2$ ($\delta = 0.14$) compound shows a deviation from the paramagnetic behavior from 100 K to the low temperatures that represents the depopulation of the fundamental state of Nd^{3+} ion, $^4I_{9/2}$, as the temperature decreases. For $x = 0.25$ and 0.3, a maximum in the susceptibility at low temperature becomes apparent. Up to a concentration of $x = 0.4$ (40% Ni^{3+}) the Nd sublattice does not order antiferromagnetically, due to the interactions of Ni and Nd sublattices. For $x = 0.8$ this order begins to disappear because there is too much Ni^{3+} created in the Ni–O planes, with low spin state, so these interactions are weakened.

On the other hand, the XANES comparison between the reduced $Nd_{2-x}Sr_xNiO_y$ samples and the nonreduced ones with the same Sr amount shows the disappearance of Ni^{3+}, the decrease of Ni^{2+}, and the increase of Ni^{+} content with increasing reduction. This increase in Ni^{+} amount would be associated with the presence of twin domains due to the different rotation axes of the NiO_6 octahedra, where the anionic vacancies are concentrated, resulting in a plane square environment for the Ni atoms. The macroscopic magnetic properties of the reduced samples change with respect to the nonreduced ones according to Ni *K*-edge XANES experiments, where a variation of the Ni oxidation state can be observed. All the reduced samples show AF order at low temperature, which varies depending on the Sr concentration and the level of reduction. A metallic Ni impurity is observed in all the reduced samples.

ACKNOWLEDGMENT

This work has been supported by CICyT under Contracts MAT96/0395CP and No. MAT97/0725.

REFERENCES

1. D. J. Buttrey, J. M. Honig, and C. N. R. Rao, *J. Solid State Chem.* **64,** 287 (1986).
2. J. Rodríguez-Carvajal, M. T. Fernández-Díaz, J. L. Martínez, F. Fernández, and R. Sáez-Puche, *Europhys. Lett.* **11,** 261 (1990).
3. R. Sáez-Puche, J. L. Rodríguez, and F. Fernández, *Inorg. Chim. Acta* **140,** 151 (1987).
4. J. M. Alonso, Ph. D. thesis, Universidad Complutense de Madrid, 1993.
5. P. Kuiper, J. van Elp, G. A. Sawatzky, A. Fujimori, S. Hosoya, and D. M. de Leeuw, *Phys. Rev. B* **44,** 4570 (1991).
6. Z. Tan, S. M. Heald, S. W. Cheong, A. S. Cooper, and A. R. Moodenbaugh, *Phys. Rev. B* **47,** 12365 (1993).
7. B. W. Arbuckle, K.V. Ramanujachary, Z. Zhang, and M. Greenblatt, *J. Solid State Chem.* **88,** 278 (1990).
8. J. L. Martínez, J. M. Alonso, M.T. Fernández-Díaz, J. Rodríguez-Carvajal, M. Vallet-Regí, and J. González-Calbet, *Physica C* **235–240,** 1561 (1994).
9. S.M. Doyle, M.P. Sridharkumar, and D. M°K Paul, *J. Phys.: Condens. Matter* **4,** 3559 (1992).
10. J. E. Greedan, G. Liu, B.W. Arbuckle, K.V. Ramanujachary, and M. Greenblatt, *J. Solid State Chem.* **97,** 419 (1992).

11. M. Medarde, J. Rodríguez-Carvajal, M. Vallet-Regí, J. Gonzalez-Calbet, and J. Alonso, *Phys. Rev. B* **49,** 8591 (1994).
12. M. Medarde. Ph.D. thesis, Universidad de Barcelona, 1992.
13. M. Medarde, J. Rodríguez-Carvajal, B. Martínez, X. Batlle, and X. Obradors, *Phys. Rev. B* **49,** 9138 (1994).
14. M. Jiménez-Ruiz, C. Prieto, A. de Andrés, J. L. Martínez, J. M. Alonso, M. Vallet-Regí, and J. M. González-Calbet, *J. Phys. IV* (*France*), **7,** C2–1203 (1997).
15. J. L. García-Múñoz, J. Rodríguez-Carvajal, P. Lacorre, and J. B. Torrance, *Phys. Rev. B* **46,** 4414 (1992).
16. J. García, J. Blasco, M. G. Proietti, and M. Benfatto, *Phys. Rev. B*, **52,** 15823 (1995).
17. M. Medarde, A. Fontaine, J. L. García-Muñoz, J. Rodríguez-Carvajal, M. de Santis, M. Sacchi, G. Rossi, and P. Lacorre, *Phys. Rev. B* **46,** 14975 (1992).
18. X. Batlle, X. Obradors, and B. Martínez, *Phys. Rev. B* **45,** 2830 (1992).
19. J. García, M. Benfatto, C. R. Natoli, A. Bianconi, A. Fontaine, and H. Tolentino, *Chem. Phys.* **132,** 295 (1989).
20. L. R. Furenlid, M. W. Renner, and E. Fujita, *Physica B* **208–209,** 739 (1995).